Excitation Waves on Cylindrical Surfaces: Rotor Competition and Vortex Drift

Oliver Steinbock

Florida State University, Department of Chemistry, Tallahassee, Florida 32306-3006

(Received 13 June 1996)

An experimental technique for preparation and image reconstruction of excitation waves in cylindrical Belousov-Zhabotinsky media is developed. It is found that pairs of spiral rotors generate ring-shaped waves by wave collisions which occur approximately 180° behind the pacemakers. Numerical simulations reveal radius-dependent competition between common vortices and rotating planar waves. This master/slave dynamics can give rise to a topology-induced spiral drift along helical loopy lines which is not due to meandering or curvature-induced changes in wave velocity. [S0031-9007(96)02162-X]

PACS numbers: 82.40.Ck, 82.20.Mj, 82.20.Wt

Propagating waves of excitation belong to the most striking phenomena in nonlinear reaction-diffusion systems [1]. They occur in a variety of biological, chemical, and physico-chemical media as diverse as cardiac tissue [2], slime mold populations [3], and catalytic surfaces [4]. Recently, questions related to wave dynamics in confined domains, such as rings [5], small disks [6], curved surfaces [7], and three-dimensional media [8] have caught more and more attention, possibly because of their relevance for some biophysical systems [2,9]. Rotating waves on curved surfaces are of particular interest, since nonuniformly curved surfaces can induce effects such as frequency changes or drift of spiral waves [10,11].

This Letter presents results on wave propagation on uniformly curved cylindrical surfaces. Experimental procedures are presented and demonstrated for the example of rotating spirals in the Belousov-Zhabotinsky (BZ) medium [12]. In contrast to spatially infinite two-dimensional media, cylindrical surfaces support not only the rotation of spirals but also the rotation of planar solitary waves. The interaction between both rotors, resulting in master/slave dynamics (i.e., suppression of slow pacemakers by fast pacemakers) and vortex drift are discussed on the basis of numerical simulations. The effects described here are not caused by curvature-dependent changes in propagation velocity, but reveal novel phenomena which should be also of importance for other surfaces (e.g. tori).

The cylindrical reaction medium was prepared as follows. A round glass tube (inner diameter 5.8 mm) was filled with hot agarose gel (Fluka; 4% w/v). While the agarose was still liquid, a glass rod (diameter 5.0 mm) was inserted and centered in the tube. After gelation the rod was carefully removed. The resulting cylindrical gel layer was then loaded with the following BZ solution: $[NaBrO_3] = 0.35$ M, $[MA] = 0.3$ M, $[H_2SO_4] = 0.35$ M, and $[\text{Ferroin}] = 10$ mM. After the concentrations in the solution and the gel reached equal values, the solution was removed from the system (dilution factor 1:4).

For reconstructing the wave locations on the cylindrical surface in terms of the spatial coordinate z, the angle ϕ, and the elapsed time t, the following procedure was developed: The probe was rotated with a constant angular frequency ω (typically 0.3 Hz) frequencies around its central axis (coincides with the z axis). Lines along the z axis were digitized with a sampling rate of 0.16 s. The resulting binary data form an array I_{nm} with n, m representing the experimental coordinates z and Φ of the reaction system, respectively. Notice that a 360° scan of the surface requires the time $2\pi/\omega$ for completion. Hence, the experimental coordinate Φ is related to the elapsed experimental time t by $\Phi = \omega t$ (for clarity the rotation angle Φ is distinguished from the time-independent "pure" cylinder coordinate ϕ).

Figure 1 shows a typical example of the described procedure as a (z, Φ) plot of local intensities. The plot reveals a pair of counterrotating spirals located at approximately $z = 1$ cm and $\Phi = n \times 360°$ that slowly expands in the course of time. Additional waves (at low z values) emanate from a pacemaker outside the observation area.

Based on the data recorded in (z, Φ) plots the original cylindrical geometry of the excitable system can be reconstructed. Figure 2 shows the wave structure of the $2600° \geq \Phi > 2960°$ interval of Fig. 1 in a three-dimensional representation, with the subfigures 2(a) and 2(b) differing only in their relative points of view. The spiral pair emits ringlike wave segments into the top part of the cylinder, which is an intrinsic feature for pacemakers on cylindrical surfaces: In an ideal experiment (without additional wave sources) a pacemaker generates waves that collide at iso-z level 180° "behind" their source. This phenomenon causes the wave structure to transform into two rings propagating toward $z \rightarrow \pm\infty$, respectively. An additional feature that cannot be found in flat two-dimensional media are solitary planar waves which extend along the z axis and are therefore periodic wave structures. Their characteristics and interaction with spiral waves (or vortices) are discussed below on the basis of numerical simulations. The presented approach should allow analogous experimental investigations. These require however, smaller cylinder radii, which makes the preparation of the gel layer difficult.

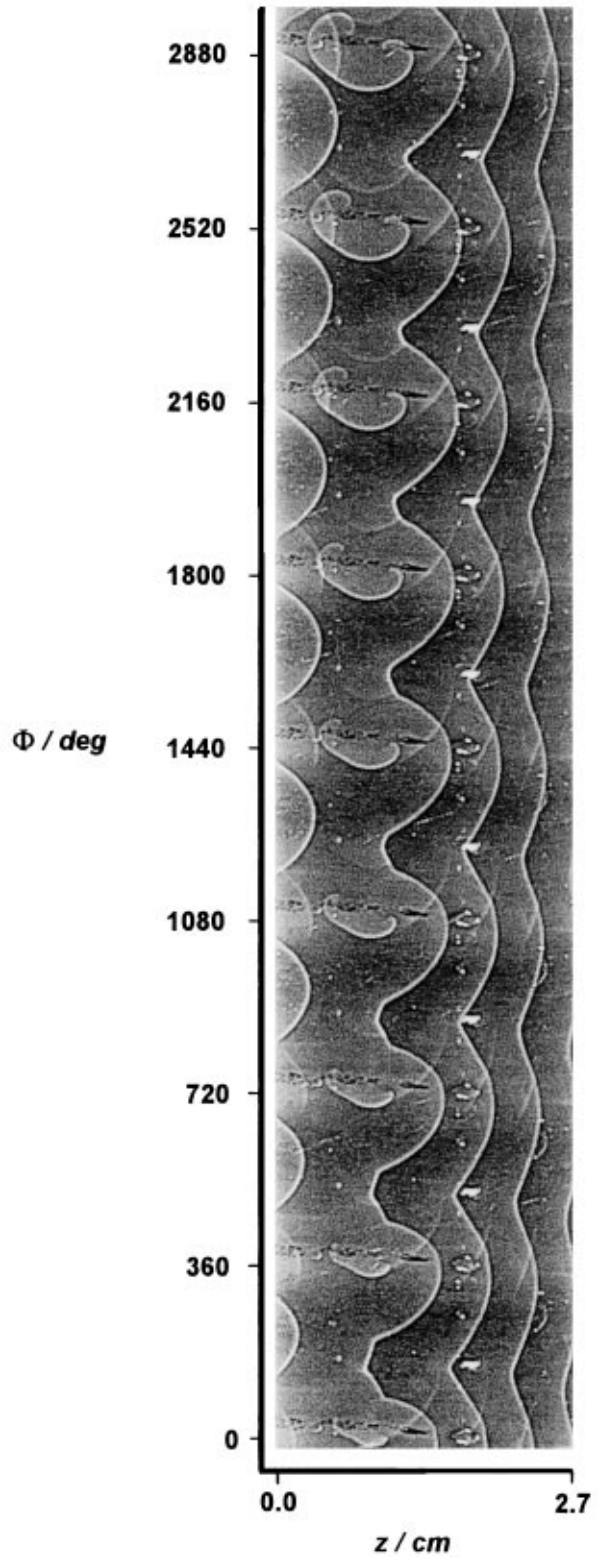

FIG. 1. Spatiotemporal evolution of a pair of spiral waves rotating on a cylindrical surface shown in terms of the experimental coordinates z (long axis) and Φ (rotation angle). According to the rotation of the probe, the spirals appear repetitively, revealing different phases of their pivoting motion. Data were obtained approximately 30 min after preparation of the system. Spirals nucleated spontaneously.

Calculations are based on the Tyson-Fife model [13],

$$\dot{u} = D_u \Delta u + \varepsilon^{-1}[u - u^2 - f\nu(u - q)/(u + q)], \quad (1)$$

$$\dot{\nu} = D_\nu \Delta \nu + u - \nu, \quad (2)$$

where u and ν describe the scaled concentrations of $HBrO_2$ and ferriin, respectively. The parameters $\varepsilon = 0.1$, $f = 2.0$, and $q = 0.002$ define an oscillatory medium in which the tips of spiral waves have simple circular trajectories (diffusion coefficients: $D_u = 1.0$ and $D_\nu = 0.6$). In the following, space and time units are denoted as su and tu, respectively. Since the gel employed in the experiments had no-flux boundary conditions in r direction and by considering the gel to be of infinitesimal small thickness, we can formulate the Laplacian in terms of cylinder coordinates (r, ϕ, z) as

$$\Delta c = r^{-2}\partial^2 c/\partial\phi^2 + \partial^2 c/\partial z^2. \quad (3)$$

Spiral waves were generated from the steady-state system by setting a strip [four grid points wide and half the system length $(L_z/2)$ long] to $u = 0.4$ and a neighboring strip to $v = 0.05$. This initial condition creates a planar wave with a tip that starts to form the desired rotating vortex. While in an ordinary plane, a rotating spiral would ultimately cover the entire system, the planar wave segment extending in z direction becomes a competitor on cylindrical surfaces. This effect is demonstrated in Fig. 3(a) showing the superposition of six consecutive snapshots as found nine spiral periods after initiation. The cylinder is divided into two distinct regions with one area ($z > 50$)

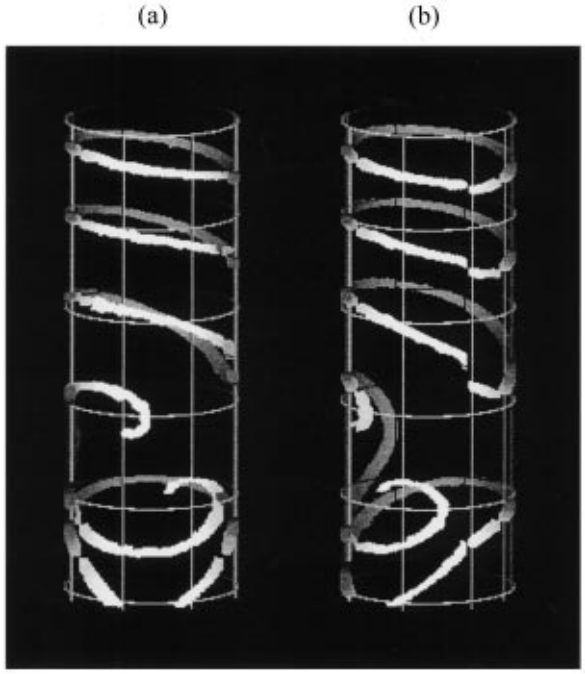

FIG. 2. Cartesian reconstruction of the cylindrical medium based on the data presented in Fig. 1. The vertical direction in this figure coincides with the (horizontal) z axis of Fig. 1 and shows the same snapshot from different points of view. The ring-shaped waves, propagating toward the top of the cylinder, are emitted by the spiral pair.

dominated by the ringlike waves emitted by the spiral and the second ($z < 50$) controlled by the planar wave. The rotation center of the spiral wave appears as a dark region close to $z = 50$. Furthermore, the second snapshot (indicated by white arrows) shows a collision between spiral tip and planar wave. This collision occurred periodically and is characteristic for the spatiotemporal evolution of this wave structure in the given medium.

A detailed trajectory of the spiral tip is presented in Fig. 3(b) for a cylinder circumference of $L = 17.5$ su. The tip location was defined via the maximal absolute value of the cross product $|\text{grad}(u) \times \text{grad}(\nu)|$ [14]. A pronounced drift of the spiral tip was found for this cylindrical geometry. In the context of the three-dimensional Cartesian space, the geometry-induced drift [Fig. 3(b)] occurs along a helical loopy line, moving the vortex around the cylinder toward the upper z boundary. Initially, the trajectory shows small transient perturbations, which are followed by a steady motion with constant drift velocity and period (in this example: $z_{\text{drift}} = 7.5$ su, $T_{\text{drift}} = 31$ tu with respect to a 360° drift). Notice, that this geometry-induced drift is not caused by the meandering instability [14], because for the given parameters the tip trajectory is circular in sufficiently large plane systems.

Vortex drift does not occur necessarily in cylindrical systems. While the rotation period of spiral waves is a characteristic value determined by the system parameters, the rotation period of planar waves extending along the z axis strongly depends on the circumference of the cylinder. Figure 4 shows the dispersion curve of the investigated system, relating the rotation period T_p of these solitary planar waves with the cylinder circumference L. The plot reveals three major dynamic modes: Below $L \approx 10$ su no stable excitation waves could be initiated and phase-locked bulk oscillations were found. Between 10 su and approximately 26 to 28 su proper excitation waves were generated that—with increasing values of L—gradually transformed into phase waves. The dashed line at $T_{\text{sp}} = 5.3$ tu indicates the characteristic rotation period of spiral waves. T_{sp} is therefore *not* the smallest period supported by the cylindrical medium introducing the possibility of competition between planar and spiral waves.

The space-time plots shown in Fig. 5 demonstrate the two major scenarios resulting from this competition. Plots were generated by collecting consecutive cuts $u(z)$ for an arbitrary but constant ϕ value. These cuts were then piled up to give the presented $u(z, t)$ plot. Figures 5(a) and 5(b) correspond to calculations obtained with $L = 25.5$ and 17.5 su, respectively, and give typical examples for the dynamics observed under $T_{\text{sp}} < T_{\text{pl}}$ (a) and $T_{\text{sp}} > T_{\text{pl}}$ (b). While planar waves extending in the z direction appear as horizontal lines in the space-time plot $u(z, t)$, spirals generate diagonal (or even V-shaped) segments. In the situation of Fig. 5(a), the spiral gains control of the entire system within approximately nine periods and removes the planar wave rotor completely. In addition, no drift of the spiral was detected. Figure 5(b), however,

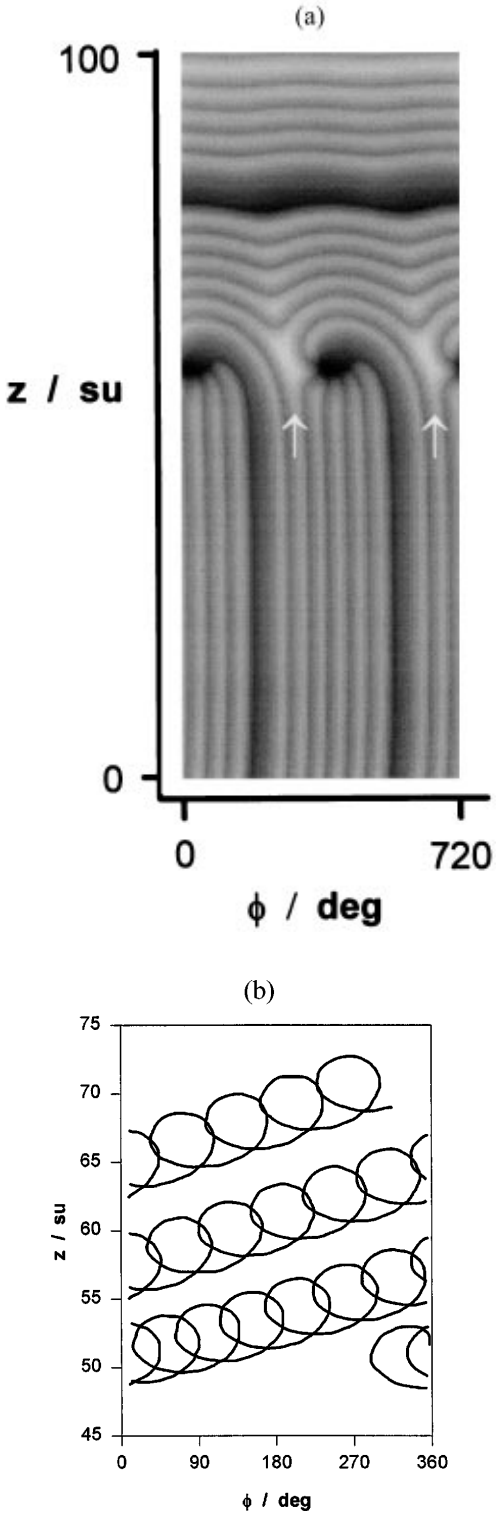

FIG. 3. Simulations demonstrating the competition between spiral and planar wave rotors on a cylindrical surface and the resulting spiral drift. (a) Superposition of six consecutive snapshots of $u(x, y)$ (time interval $\Delta\tau = 0.66$ tu) with white arrows indicating the second snapshot. (b) Trajectory of the drifting spiral tip. Parameters used for both calculations: System length in z direction $L_z = 100$; grid spacing of z and arclength s: $\Delta z = \Delta s = 0.25$; time step $\Delta t = 0.001$. The Laplacian was calculated using a nine-point formula.

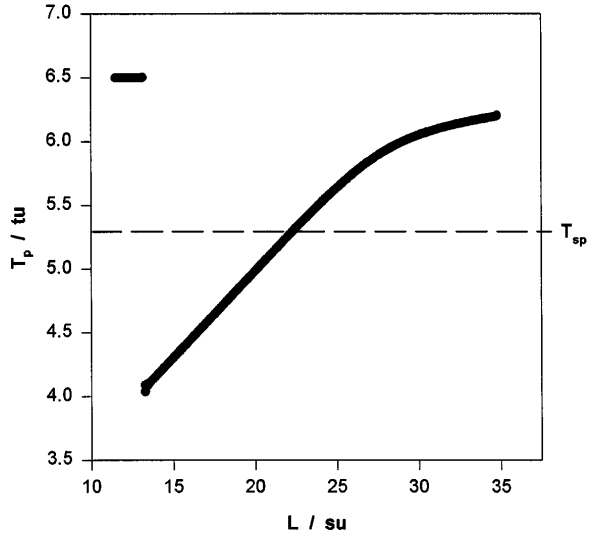

FIG. 4. Dispersion curve of the system relating the rotation period T_p of planar rotors to the circumference L of the cylinder. The period of 6.5 tu corresponds to the intrinsic oscillation period of the system (bulk oscillations). The dashed line indicates the rotation period of spiral waves as found in large flat two-dimensional systems. Data were obtained from simulations of one-dimensional ring-shaped media with $\Delta t = 0.001$ and $\Delta s = 0.1$.

shows a slow process of planar wave expansion, thus removing the spiral. The process is accompanied by adjustments in local frequency: Due to the different periods of spiral and planar rotor several waves vanish. This effect occurs during the drift of the vortex core across the analyzed line of constant ϕ value. The described master-slave scenario and its characteristic spiral drift could also be of interest for certain biophysical systems [2,3,9].

The author thanks N. Dalal for his support and hospitality and B. Neumann for discussions. This work was supported by the Fonds der Deutschen Chemischen Industrie.

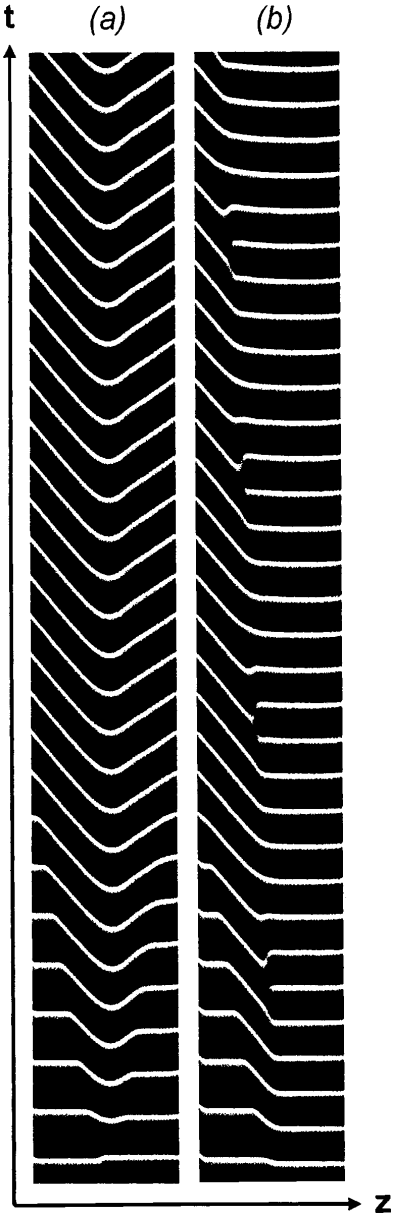

FIG. 5. Space-time plots $u(z,t)$ generated along a line of constant ϕ value. The plots demonstrate the two major scenarios of competition between spiral and planar wave rotors: (a) Suppression of the planar wave by the spiral: $L = 25.5$; (b) slaving of the spiral by the planar wave with resulting drift of the vortex tip: $L = 17.5$.

[1] Focus issue on From Oscillations to Excitability—A Case Study in Spatially Extended Systems, edited by S. C. Müller, P. Coullet, and D. Walgraef [Chaos **4**, 439–568 (1994)].
[2] J. M. Davidenko *et al.,* Nature (London) **355**, 349 (1992).
[3] O. Steinbock, F. Siegert, S. C. Müller, and C. J. Weijer, Proc. Natl. Acad. Sci. U.S.A. **90**, 7332 (1993).
[4] H. H. Rotermund, S. Jakubith, A. von Oertzen, and G. Ertl, Phys. Rev. Lett. **66**, 3083 (1991).
[5] M. A. Liauw, J. Ning, and D. Luss, J. Chem. Phys. **104**, 5657 (1996).
[6] V. A. Davydov and V. S. Zykov, JETP **76**, 414 (1993); N. Hartmann *et al.,* Phys. Rev. Lett. **76**, 1384 (1996); M. Gómez-Gesteira *et al.,* Phys. Rev. E **53**, 5480 (1996).
[7] J. Maselko and K. Showalter, Nature (London) **339**, 609 (1989); P. Grindrod and J. Gomatam, J. Math. Biol. **25**, 597 (1987).
[8] B. J. Welsh, J. Gomatam, and A. E. Burgess, Nature (London) **304**, 611 (1983); K. I. Agladze, R. A. Kocharyan, and V. I. Krinsky, Physica (Amsterdam) **49D**, 1 (1991).
[9] A. T. Winfree, *When Time Breaks Down* (Princeton University Press, Princeton, NJ, 1987).
[10] P. K. Brazhnik, V. A. Davydov, and A. S. Mikhailov, Theor. Math. Phys. **74**, 300 (1988).
[11] V. A. Davydov and V. S. Zykov, Physica (Amsterdam) **49D**, 71 (1991).
[12] *Chemical Waves and Patterns,* edited by R. Kapral and K. Showalter (Kluwer, Dordrecht, Netherlands, 1995).
[13] See, e.g., J. P. Keener and J. J. Tyson, Physica (Amsterdam) **21D**, 307 (1986).
[14] W. Jahnke and A. T. Winfree, Int. J. Bifurcation Chaos **1**, 445 (1991).